Transp Porous Med (2009) 80:345–371
DOI 10.1007/s11242-009-9364-7

Analysis of Laminar Flow and Forced Convection Heat Transfer in a Porous Medium

Fethi Kamışlı

Received: 29 October 2008 / Accepted: 13 February 2009 / Published online: 11 March 2009

Abstract The flow of an incompressible Newtonian fluid confined in a planar geometry with different wall temperatures filled with a homogenous and isotropic porous medium is analyzed in terms of determining the unsteady state and steady state velocities, the temperature and the entropy generation rate as function of the pressure drop, the Darcy number, and the Brinkman number. The one-dimensional approximate equation in the rectangular Cartesian coordinates governing the flow of a Newtonian fluid through porous medium is derived by accounting for the order of magnitude of terms as well as accompanying approximations to the full-blown three-dimensional equations by using scaling arguments. The one-dimensional approximate energy and the entropy equations with the viscous dissipation consisting of the velocity gradient and the square of velocity are derived by following the same procedure used in the derivation of velocity expressions. The one-dimensional approximate equations for the velocity, the temperature, and the entropy generation rate are analytically solved to determine the velocity, the temperature, and the entropy distributions in the saturated porous medium as functions of the effective process parameters. It is found that the pressure drop, the Darcy number, and the Brinkman number affect the temperature distribution in the similar way, and besides the above parameters, the irreversibility distribution ratio also affects the entropy generation rate in the similar way.

Keywords Porous medium · Darcy number · Entropy generation · Viscous dissipation · Forced convection

List of Symbols

Variables

Br Brinkman number $= Ec\ Pr$
Cp Specific heat (J $kg^{-1}\cdot K^{-1}$)
Pr Prandtl number $= C_p/k$

F. Kamışlı (✉)
Department of Chemical Engineering, Firat University, 23119 Elazig, Turkey
e-mail: fkamisli@firat.edu.tr

Ec	Eckert number $= u_m^2/Cp\Delta T$
Da	Darcy number K/h_2
F	Empirical coefficient
Fr_i	Froude number u_0^1/hg_i
h	Half transverse distance (m)
g_i	Gravity in i-direction
k_f	Thermal conductivity ($\mathrm{W \cdot m^{-1} \cdot K^{-1}}$)
K	Permeability ($\mathrm{m^2}$)
ℓ	Characteristic length in the x-direction (m)
N_{DB}	Entropy generation number, Darcy–Brinkman dissipation $= Bru^2/\Omega Da$
N_F	Entropy generation number, velocity gradient dissipation $= Br(\partial u/\partial y)^2/\Omega$
N_S	Entropy generation number, total
N_Y	Entropy generation number, conduction $= (\partial\theta/\partial y)^2$
P	Dimensionless pressure $= \tilde{P}/\left(\mu u_0 \ell/h^2\right)$
P_0	Dimensionless pressure gradient dP/dx
Re	Cross-flow Reynolds number $= \rho u_0 h/\mu$
S_G	Entropy generation rate ($\mathrm{W \cdot m^{-3} \cdot K^{-1}}$)
$S_{G,C}$	Characteristic entropy transfer rate
t	Dimensionless time $= \tilde{t}/\left(h^2\rho/\mu\right)$
T	Temperature (K)
T_0	Reference temperature (K)
T_1	Temperature at the lower plate (K)
T_2	Temperature at the upper plate (K)
$\tilde{u}$	Velocity in x-direction ($\mathrm{m \cdot s^{-1}}$)
u_0	Characteristic velocity ($\mathrm{m \cdot s^{-1}}$)
$\tilde{v}$	Velocity in y-direction ($\mathrm{m \cdot s^{-1}}$)
v_0	Characteristic velocity in y-direction ($\mathrm{m \cdot s^{-1}}$)
$\tilde{w}$	Velocity in z-direction ($\mathrm{m \cdot s^{-1}}$)
u, v, w	Dimensionless velocities
$\tilde{x}$	Axial direction
$\tilde{y}$	Transverse direction
$\tilde{z}$	Normal to the x-direction
x, y, z	Dimensionless directions

Greek Symbols

θ	Dimensionless temperature
Ω	Dimensionless temperature difference $= \Delta T/T_0$
Φ	Total viscous dissipation
μ	Dynamic viscosity ($\mathrm{Pa \cdot s}$)
ρ	Density of the fluid ($\mathrm{kg \cdot m^{-3}}$)

1 Introduction

The flow of a fluid through porous media at low Reynolds number and the heat transfer with forced or natural convections in porous media have long been important subjects of many investigations due to its importance in a variety of situations. The theoretical and

analytical studies of convection processes in porous media are scientifically interesting and technologically important. As stated, the fluid flow through porous media and heat transfer is fundamental in nature and is of great practical importance in many diverse applications, including the production of oil and gas from geological structures, the gasification of coal, the retorting of shale oil, filtration, ground-water movement, regenerative heat exchanger, surface catalysis of chemical reactions, adsorption, coalescence, drying, ion exchange, and chromatography.

Along with the advancement of science and technology, modern instruments and equipments such as micro-electromechanical system, laser coolant lines, and many compact heat exchangers have been started to be used for many purposes. The heat transfer with forced convection occurs in increasing variety of such modern instruments and equipments. There is an increased need for conserving useful energy and thus, producing thermodynamically efficient heat transfer processes in which internal forced convection heat transfer occurs.

As stated previously, the flow of fluid through porous media and forced convection at laminar flow regime has been investigated in the fields of chemical, biochemical, mechanical and environmental engineering, and science. The extensive studies performed theoretically and analytically on the topic of forced convection and free convection in porous media are given by Nield and Bejan (2006), Bejan et al. (2004), Ingham and Pop (2005), and Vafai (2005).

The laminar-forced convection in a porous medium bounded by isothermal parallel plates was analyzed by Kaviany (1985) with the use of the Brinkman-extended Darcy model. The fully developed forced convection in porous media between two parallel plates at constant heat flux was studied by Vafai and Kim (1989). The closed form solutions to Brinkman–Forchheimer-extended Darcy momentum equation and associated heat transfer equation were obtained.

Nield et al. (1996) theoretically investigated fully developed forced convection in a fluid-saturated porous-medium channel bounded by isothermal parallel plates. The momentum equation with the non-linear Forchheimer term was analytically solved to determine the effects of some dimensionless numbers. In another study, Nield et al. (2003) analyzed the heat transfer in a thermally developing region of a hydrodynamically developed flow in a isothermal parallel plate filled with porous materials. The viscous dissipation and axial heat conduction were considered in their article. They examined the effects of Brinkman, Peclet, and Darcy number on the heat transfer for different dissipation models.

Mohammad (2003) analyzed the flow field and heat transfer with laminar forced convection in conduits filled with a porous material to different degrees. He concluded that the effect of Darcy number on heat transfer in the fully developed flow region may largely be neglected for $Da > 1$ in the case of homogenously filled channel.

Haji-Sheikh and Vafai (2004) undertook a heat transfer analysis on various cross sections of conduits by determining the effect of Darcy number on the thermal performance of porous inserts. The momentum and energy equations for the heat transfer analysis on thermally developing convection in ducts of various cross sections were solved by the method of weighted residuals.

Haji-Sheikh et al. (2006) examined heat transfer in the thermal entrance region for flow through rectangular passages being either open or filled with saturated materials. They used the Green's function to solve the energy equations and their associated boundary conditions. They concluded that the thermally fully developed condition might not be attainable in practical applications for very narrow passages with prescribed wall heat flux.

Hooman et al. (2007) analytically performed the first- and the second-law characteristics of fully developed forced convection inside a porous-saturated duct of rectangular cross section. The Darcy–Brinkman momentum equation was used to describe the flow in porous media.

In this investigation, three different types of thermal boundary conditions were examined to analyze the system in terms of the Nusselt number, the Bejan number, and the dimensionless entropy generation rate. In another study, Hooman and Haji-Sheikh (2007) worked on heat transfer and entropy generation analysis of the thermally developing forced convection in a porous-saturated duct of rectangular cross section with walls that are maintained at a constant and uniform heat flux. The thermal energy equation with viscous dissipation for Brinkman flow model was solved by the extended weighted residual method. The problem was analyzed in terms of the second law of thermodynamics by determining the Nusselt number, the bulk temperature distribution, the Darcy number, and the Brinkman number.

Morosuk (2005) investigated the entropy generation due to flow in an isothermal pipe that was fully or partially filled with porous materials. The effects of porous layer thickness and permeability of layer on the rate of entropy generation were examined. The developing and fully developed flow conditions were also considered in that article.

Mahmud and Fraser (2005) worked on the thermally and hydrodynamically developed forced convection and entropy generation in a fluid-saturated porous-medium channel bounded by two parallel plates at constant, but different temperatures. The Darcy–Brinkman momentum equation was used to describe the flow in porous media. The physical properties were taken as constant, therefore the flow field is decoupled from the temperature field, and the one-dimensional transport equations were solved analytically. They also solved the Darcy–Brinkman equations numerically and the numerical and analytical results were compared with one another. Thermal asymmetry due to different wall temperatures results in an asymmetric temperature distribution in the porous gap. The problem is examined in terms of the Eckert number, the Prandtl number, and the Darcy number.

Mahmud and Fraser (2005) study was extended, by including the convective term in the axial direction to the energy equation, by Mitrovic and Maletic (2007). They numerically investigated the effect of thermal asymmetry on laminar-forced convective heat transfer in porous media bounded by two large parallel plates at constant, but different temperatures. In that article, the forced convective heat transfer for laminar flow through the porous media was analyzed in terms of the Darcy number, the Peclet number, and the Nusselt number. They concluded that reversal of the heat flux at a certain position along the flow at least at one of the wall can happen because of thermal asymmetry.

Although it is a controversial issue (Nield 2000; Al-Hadhrami et al. 2003), by considering the Navier–Stokes equation for a Newtonian fluid flow clear of solid material, the viscous dissipation in the Darcy–Brinkman momentum equation is given as follows:

$$\Phi = \frac{\mu \tilde{u}^2}{K} + \mu \left(\frac{\partial \tilde{u}}{\partial \tilde{y}} \right)^2,$$

where Φ is the viscous dissipation. As can be seen from the above equation, the viscous dissipation consists of two terms: the first term can be called as the Darcy–Brinkman dissipation and the second one can be called as the velocity-gradient dissipation for the one-dimensional flow.

In the previous studies (Mahmud and Fraser 2005 and Mitrovic and Maletic 2007), the viscous dissipation was taken as only the first term of the above equation. Mahmud and Fraser (2005) mentioned that the inclusion of the second term to the Brinkman–Darcy momentum equation was left for a future work. To the author's knowledge, to date none of the previous studies considered the whole equation for the viscous dissipation. Therefore, the goal of this study is to analyze the entropy generation due to heat conduction in the transverse direction and viscous dissipation including velocity gradient and square of velocity. Furthermore, in

this study, the one-dimensional unsteady-state and steady-state velocity equations for the saturated porous media are derived by accounting for the order of magnitude of terms as well as the accompanying approximations to the full-blown three-dimensional equations by using scaling arguments and solved analytically. Contrary to the previous studies, the different scale for pressure is used and then, the Reynolds number is eliminated from the Darcy–Brinkman momentum equation. In this context, the steady-state one-dimensional velocity equation for the saturated porous medium bounded by parallel plates is constant, but different temperatures are used to obtain analytical expressions for the steady-state temperature and thus, the steady-state entropy generation distributions as functions of the Darcy number, the Brinkman number (the Prandtl number $\times$ the Eckert number), the irreversibility distribution ratio, and the pressure drop.

2 Theoretical Analysis and Mathematical Formulation

Consider an unsteady-state and a steady-state, incompressible Newtonian fluid flowing in the axial direction in the parallel plates filled with a homogenous and isotropic porous medium. The planar geometry which is at constant, but different wall temperature consists of two closely separated large parallel plates having a distance of $2h$ between them. The sides of this rectangular channel are at a distance of $2Z_0$ apart, where $h << Z_0$ and its axial length is equal to ℓ as shown in Fig. 1.

The homogenous and isotropic porous medium between two large parallel plates is saturated with a Newtonian fluid flowing in the axial direction, and is assumed to be in the local thermodynamic equilibrium with fluid. It is assumed that the thermophysical properties of the solid matrix and of the fluid are constant. The porosity and permeability are also assumed to be constant, even near the walls (see Mahmud and Fraser 2005 and references therein). The heat transfers by natural convection and thermal radiation and in the axial direction are assumed to be negligible in the present problem.

There are two models, namely, *Local Thermal Equilibrium* model (LTE) and *Local Thermal non-Equilibrium* model (LTNE) for handling transport processes in porous media. In the LTE, the fluid and the porous medium are considered as a single phase having physical properties of the actual phases mostly weighted by the volume fractions occupied by these phases. The applicability of this model is confined to a certain range of process and system parameters like fluid velocity and transport properties of the phases. Contrary to this model, in the LTNE, the thermal interaction among the phase within the porous system is assumed to exist. According to this model, the thermal interaction is based on a heat transfer coefficient at the interface within the porous system, which is previously unknown. In the LTNE, the two equations model is usually considered to be more adequate than the one equation LTE model (see Mitrovic and Maletic 2007 and references therein).

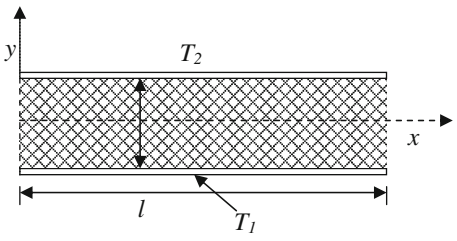

Fig. 1 Schematic diagram of the saturated porous medium between two parallel plates

In this study, the LTE is used for treating transport processes in porous media as in the previous studies (Mahmud and Fraser 2005; Mitrovic and Maletic 2007).

In order to derive the one-dimensional equation describing a Newtonian fluid flow between the parallel plates filled with the homogenous and isotropic porous medium, a full three-dimensional equation of the continuity and the equations of the motion with the Forchheimer and the Darcy–Brinkman terms are written in the dimensional form and these equations are non-dimensionalized by introducing dimensionless variables. After obtaining the dimensionless form of the equations, the order of magnitude of the terms is used to simplify the equations of continuity and motion. Finally, the desired one-dimensional equation describing the flow of a Newtonian fluid confined between parallel plates filled with the homogenous and isotropic porous medium is derived by using an approximate form of the velocity field for this geometry.

The cross-sectional area is constant, and the height and length of the channel are denoted as $2h$ and ℓ, respectively. In order to obtain the dimensionless continuity and the Darcy–Brinkman momentum equations, dimensionless variables are defined as

$$x = \frac{\tilde{x}}{\ell}, \quad y = \frac{\tilde{y}}{h}, \quad z = \frac{\tilde{z}}{\ell}, \quad u = \frac{\tilde{u}}{u_0}, \quad v = \frac{\tilde{v}}{v_0\,(h/\ell)^2},$$
$$w = \frac{\tilde{w}}{u_0 h/\ell}, \quad P = \frac{\tilde{P}}{\mu u_0 \ell/h^2}, \quad t = \frac{\tilde{t}}{h^2\rho/\mu},$$

where ℓ is the length of the parallel plates, h is the half distance between the two plates, u_0 is the characteristic velocity in the x-direction, and u, v, w are the velocities in the x-, y-, and z-directions. Since the dominant flow occurs in the axial direction, from the momentum balance in this direction, the pressure is scaled by the term of $\mu u_0 \ell/h^2$. The velocity components in the cross-sectional plane are scaled according to the conservation of mass in the geometry. The characteristic velocities in the y- and z-directions were chosen to be proportional with the characteristic velocity in the axial direction since it is intuitively expected that the characteristic velocity in the x-direction is larger than that in the z-direction, which is larger than that in the y-direction. By using the dimensionless variables defined above, the dimensionless continuity equation is given by

$$\frac{\partial u}{\partial x} + \frac{\ell}{h}\left(\frac{\partial v}{\partial y} + \frac{\partial w}{\partial z}\right) = 0. \tag{1}$$

For a typical parallel-plate geometry, the half height of geometry h is quite small with respect to the characteristic length of the channel ℓ and thus, the coefficient of the second term in Eq. 1 h/ℓ is much less than unity and the changes in dimensionless quantities take place over dimensionless length scales of the order of unity.

The dimensionless Darcy–Brinkman momentum equations in the x-, y-, and z-directions are, respectively, given as follows:

$$\frac{\partial u}{\partial t} + Re\delta\left[u\frac{\partial u}{\partial x} + \delta v\frac{\partial u}{\partial y} + \delta w\frac{\partial u}{\partial z}\right] + Re\frac{Fu^2}{\sqrt{Da}} = -\frac{\partial P}{\partial x} + \delta^2\frac{\partial^2 u}{\partial x^2} + \frac{\partial^2 u}{\partial y^2} + \delta^2\frac{\partial^2 u}{\partial z^2} - \frac{u}{Da} + G_x \tag{2}$$

$$\delta^3\left[\frac{\partial v}{\partial t}+Re\delta\left(u\frac{\partial v}{\partial x}+\delta v\frac{\partial v}{\partial y}+\delta w\frac{\partial v}{\partial z}+\delta\frac{Fv^2}{\sqrt{Da}}\right)\right]=-\frac{\partial P}{\partial y}+\delta^3\left[\delta\frac{\partial^2 v}{\partial x^2}+\frac{\partial^2 v}{\partial y^2}+\delta\frac{\partial^2 v}{\partial z^2}\right]-\delta^2\frac{v}{Da}+\delta G_y \quad (3)$$

$$\delta\left[\frac{\partial w}{\partial t}+Re\left(u\delta\frac{\partial w}{\partial x}+v\delta^2\frac{\partial w}{\partial y}+\delta^2 w\frac{\partial w}{\partial z}+\delta\frac{Fw^2}{\sqrt{Da}}\right)\right]=-\frac{\partial P}{\partial z}+\delta\left[\delta^2\frac{\partial^2 w}{\partial x^2}+\frac{\partial^2 w}{\partial y^2}+\delta^2\frac{\partial^2 w}{\partial z^2}-\frac{w}{Da}\right]+G_z, \quad (4)$$

where

$$\delta=\frac{h}{\ell},\quad Re=\frac{\rho u_0 h}{\mu},\quad G_x=\frac{Re}{Fr_x},\quad G_y=\frac{Re}{Fr_y},$$
$$G_z=\frac{Re}{Fr_z},\quad Fr_i=\frac{u_0^2}{hg_i},\quad Da=\frac{K}{h^2}$$

g_i denotes the component of gravity in the i-direction, Fr_i stands for the Froude number in the i-direction, and F the empirical coefficient, which is usually very small. Re and Da are the Reynolds number and the Darcy number, respectively.

The dimensionless continuity and Darcy–Brinkman momentum equations given above can be simplified by considering the order of magnitudes of terms, i.e., for a typical parallel-plate geometry, in general, the cross-sectional half height of the parallel plates, h is much smaller than its length ℓ. Consequently, the parameter δ is much less than unity as stated previously. Thereby, as $\delta \to 0$, the equation of continuity becomes

$$\frac{\partial u}{\partial x}=0. \quad (5)$$

The above expression shows that the velocity in the axial direction is constant and the primary motion is in the x-direction due to the pressure gradient in this direction in the parallel plates. This can be also seen intuitively since a purely viscous Newtonian fluid does not move in the y- and z-directions when the pressure drop is exerted in the axial direction.

On the other hand, as $\delta \to 0$, the Darcy–Brinkman momentum equations in y- and z-direction become

$$\frac{\partial P}{\partial y}=0 \quad (6)$$

$$\frac{\partial P}{\partial z}=G_z. \quad (7)$$

Since the gravitational force in the z-direction is zero, the Froude number in this direction becomes infinity, which makes G_z be equal to zero. Therefore, Eqs. 6 and 7 indicate that the pressure drops are independent of y and z. In other words, the pressure has to be a function of the axial direction only. By taking $Re << 1$ and $\delta \to 0$, for typical laminar flow regime and typical parallel plates, respectively, the equation of momentum in the axial direction reduces to the following equation:

$$\frac{\partial u}{\partial t}=-\frac{\partial P}{\partial x}+\frac{\partial^2 u}{\partial y^2}-\frac{u}{Da}. \quad (8)$$

Equation 8 is the dimensionless unsteady-state Darcy–Brinkman momentum equation in the axial direction for the parallel plates filled with the homogenous and isotropic porous

medium. As seen from Eq. 8, the velocity is dependent on t and y. Thus, the solution can be decomposed into two parts, namely, a transient part and a steady-state part, $u = u_t + u_S$ (Kamışlı 2008; Fang 2004). Thereby, Eq. 8 can turn out to be two separated problems.

3 Analytical Solution

We consider a Newtonian fluid confined in two large parallel plates filled with the homogenous and isotropic porous medium. In order to solve the given set of Eqs. 5–8, the required time- and spatial-dependent velocity boundary conditions are specified as follows:

$$u(t, \pm 1) = 0, \quad \partial u/\partial y(t, 0) = 0 \quad \text{and} \quad u(0, y) = 0. \tag{9}$$

Equations 5–9 are the set of approximate algebraic and ordinary differential equations that govern the pressure-driven flow of a Newtonian fluid in the parallel plates filled with the homogenous and isotropic porous medium. The velocity distribution and thus the volumetric flow rate per unit width in the geometry can be obtained by solving Eq. 8 that is linear ordinary differential equation and can be analytically solved by the method of separation of variables. In fact, it can be also solved with the aid of the Laplace transformation. In solution of Eq. 8 one approach expands the velocity in a series of complementary error function (see Schlicting and Gersten 2000), while another is to use the standard trigonometric Fourier series, which satisfies the governing equation. The set of Eqs. 5–9 includes the effects of inertia with the time-dependent term and the Darcy–Brinkman term. The one-dimensional governing equation for the parallel plates can be obtained by integrating Eq. 8 across the cross-sectional area of parallel plates per unit width. Equation 8 subject to the boundary conditions given by Eq. 9 is solved by decomposing it into two parts, namely, a transient part and a steady-state part, $u = u_t + u_s$, where indices t and S denote transient and steady-state solutions, respectively. Then, the two separate problems are obtained, and the steady-state part of Eq. 8 and the related boundary conditions are, respectively, given as follows:

$$\frac{\partial^2 u_S}{\partial y^2} - \frac{u_S}{Da} = \frac{\partial P}{\partial x} \tag{10}$$

$$u_S = 0 \quad \text{at} \quad y = \pm 1, \quad \frac{\partial u_S}{\partial y} = 0 \quad \text{at} \quad y = 0. \tag{11}$$

Equation 10 with the different form was given by Mahmud and Fraser (2005) and Mitrovic and Maletic (2007). In those studies, the Reynolds number lies as a multiplier of pressure gradient; then, the steady-state velocity becomes functions of the Reynolds number, the Darcy number, and the transverse distance and in turn, the Reynolds number, as known, is a function of velocity. The difference, in terms of the arrangement of the simplified Darcy–Brinkman momentum equation, between this study and the previous studies (Mahmud and Fraser 2005; Mitrovic and Maletic 2007) comes from the different scale factors used for non-dimensionalizing pressure.

The characteristic pressure (scale factor for pressure) is not independent of other characteristic quantities. It is well known that if inertial effects dominate and losses are small, the pressure is of the order of an inertial force ρu^2 that was used as a characteristic pressure in the previous investigations (Mahmud and Fraser 2005; Mitrovic and Maletic 2007). When the viscous terms are much more important than the inertial terms, we know that the pressure is of the order of a characteristic viscous force $\mu u/h$ that is modified and used as a characteristic pressure in this study.

When inertial and viscous terms are of comparable magnitude, then either form of the characteristic pressure may be used (Denn 1980).

The solution of Eq. 10 subject to the boundary conditions given by Eq. 11 can be obtained as

$$u_S = -DaP_0\left(1 - \frac{\exp(y/\sqrt{Da}) + \exp(-y/\sqrt{Da})}{\exp(1/\sqrt{Da}) + \exp(-1/\sqrt{Da})}\right), \tag{12}$$

where $P_0 = \partial P/\partial x$. Equation 12 is the analytical solution of Eq. 8 at the steady-state condition. As can be seen from the above equation, the steady-state velocity depends on the Darcy number, the pressure gradient, and the transverse distance. If Eq. 12 is considered for the limiting values of the Darcy number, unfortunately one cannot recover Poiseuille solution from that equation as $Da \to \infty$ (that corresponds to the case of a fluid clear of solid material). In fact, as $Da \to \infty$ in Eq. 12, the steady-state velocity goes to zero, which is an unrealistic value. For the case of $Da \to \infty$ the steady-state velocity can be obtained from Eq. 10 by comparing the first and the second terms on the left-hand side. The second term on the left-hand side of Eq. 10 goes to zero as $Da \to \infty$, and the solution of the resulting equation is given as follows:

$$u_S = -\frac{1}{2}P_0\left[1 - y^2\right]. \tag{13}$$

The above expression is the same as the velocity of Poiseuille flow of a Newtonian fluid confined in parallel plates. Note that contrary to the previous studies (Mahmud and Fraser 2005; Mitrovic and Maletic 2007), Eqs. 12 and 13 do not contain the Reynolds number.

Substituting equation of $u(t, y) = u_t(t, y) + u_S(y)$ into Eqs. 8 and 9 gives the following linear ordinary differential equation and the boundary and the initial conditions, respectively.

$$\frac{\partial u_t}{\partial t} = \frac{\partial^2 u_t}{\partial y^2} - \frac{u_t}{Da} \tag{14}$$

$$u_t(t, y) = 0 \quad \text{at} \quad y = \pm 1, \quad \frac{\partial u_t(t, y)}{\partial y} = 0 \quad \text{at} \quad y = 0 \tag{15a}$$

$$u_t(0, y) = DaP_0\left(1 - \frac{\exp(y/\sqrt{Da}) + \exp(-y/\sqrt{Da})}{\exp(1/\sqrt{Da}) + \exp(-1/\sqrt{Da})}\right). \tag{15b}$$

The solution of Eq. 14 subject to the boundary and the initial conditions given by Eq. 15 can be accomplished by the method of separation of variables, which is given as

$$u_t = \psi(t)\phi(y), \tag{16}$$

where ψ and ϕ are dimensionless functions. Substituting Eq. 16 into Eq. 14 and separating according to the variables results in the following two ordinary differential equations.

$$\psi' + (1/Da + \lambda)\,\psi = 0 \tag{17a}$$

$$\phi'' + \lambda\phi = 0. \tag{17b}$$

The prime over the variable denotes a derivative of that variable with respect to an independent variable in it. The boundary conditions for Eq. 17b become $\phi\,(\pm 1) = 0$ and $\partial\phi/\partial y = 0$ at $y = 0$. Therefore, the solution of Eq. 14 by the method of separation variables can be obtained as

$$u_t = \sum_{n=1}^{\infty} \left(\frac{4DaP_0(-1)^{n-1}}{(2n-1)\pi} - \frac{DaP_0(2n-1)\pi}{1/Da + (2n-1)^2\pi^2/4} \sin((n-1/2)\pi y) \right.$$
$$\times \frac{\cosh(y/\sqrt{Da})}{\cosh(1/\sqrt{Da})} - \frac{2\sqrt{Da}P_0}{1/Da + (2n-1)^2\pi^2/4} \cos((n-1/2)\pi y) \frac{\sinh(y/\sqrt{Da})}{\cosh(1/\sqrt{Da})} \Bigg)$$
$$\times \exp(-(1/Da + (2n-1)^2\pi^2/4)t) \cos((n-1/2)\pi y). \quad (18)$$

Equation 18, which is an analytical solution of the transient part of Eq. 8, gives the velocity distribution as functions of the dimensionless time, the dimensionless transverse distance, the dimensionless pressure gradient, and the Darcy number. The overall transient solution for the flow of a Newtonian fluid confined in the parallel plates filled with a homogenous and isotropic porous medium is obtained by considering Eq. 12 and 18 with the equation of $u(t, y) = u_t(t, y) + u_S(y)$ as follows:

$$u(t, y) = -DaP_0 \left(1 - \frac{\exp(y/\sqrt{Da}) + \exp(-y/\sqrt{Da})}{\exp(1/\sqrt{Da}) + \exp(-1/\sqrt{Da})} \right) + \sum_{n=1}^{\infty} \exp(-(1/Da$$
$$+ (2n-1)^2\pi^2/4)t) \cos((n-1/2)\pi y) \left(\frac{4DaP_0(-1)^{n-1}}{(2n-1)\pi} \right.$$
$$- \frac{DaP_0(2n-1)\pi}{1/Da + (2n-1)^2\pi^2/4} \sin((n-1/2)\pi y) \times \frac{\cosh(y/\sqrt{Da})}{\cosh(1/\sqrt{Da})}$$
$$\left. - \frac{2\sqrt{Da}P_0}{1/Da + (2n-1)^2\pi^2/4} \cos((n-1/2)\pi y) - \frac{\sinh(y/\sqrt{Da})}{\cosh(1/\sqrt{Da})} \right). \quad (19)$$

Here, we followed a more systematic approach, namely, the order of magnitude of each term in each equation for the derivation of the one-dimensional approximate governing equation of a Newtonian fluid flow in the parallel plates filled with the homogenous and isotropic porous medium, and the resulting equation (Eq. 8) is solved by using the method of separation of variables subject to the boundary conditions given by Eq. 9.

Note that one cannot recover the unsteady-state velocity expression valid for a flow of a Newtonian fluid confined in a parallel plate, as $Da \to \infty$. Darcy number (Da) is a measure of the relative permeability of the porous media. In other words, large values of Darcy number correspond to a fluid flow in a medium clear of solid material. Again, the magnitude of terms in Eq. 8 has to be evaluated as $Da \to \infty$, and the resulting equation has to be solved to obtain the unsteady-state velocity expression in the case of $Da \to \infty$. For the case of $Da \to \infty$, Eq. 8 can be rewritten as follows:

$$\frac{\partial u}{\partial t} = -\frac{\partial P}{\partial x} + \frac{\partial^2 u}{\partial y^2} \quad (20)$$

By following the same procedure outlined above, the solution of Eq. 20 is given as follows:

$$u_t = \sum_{n=1}^{\infty} \exp\left(-\left((2n-1)^2\pi^2/4\right)t\right) \cos\left((n-1/2)\pi y\right) \left(\frac{2P_0(-1)^{n-1}}{(2n-1)\pi} - \frac{8P_0 y}{(2n-1)^2\pi^2} \right.$$
$$\left. \times \cos\left((n-1/2)\pi y\right) - 2P_0 \left(\frac{y^2}{(2n-1)\pi} - \frac{8}{(2n-1)^3\pi^3} \right) \sin\left((n-1/2)\pi y\right) \right). \quad (21)$$

Equation 21, which is an analytical solution of the transient part of Eq. 8, gives the velocity distribution as functions of the dimensionless time, the transverse distance, and the dimensionless pressure gradient as $Da \to \infty$. For the case of $Da \to \infty$, the overall transient solution for the flow of a Newtonian fluid confined in the parallel plates filled with a homogenous and isotropic porous medium is obtained by considering Eq. 13 and 21 with the equation of $u\,(t, y) = u_t(t, y) + u_S(y)$ as follows:

$$u = -\frac{1}{2}P_0\left[1 - y^2\right] + \sum_{n=1}^{\infty} \exp\left(-\left((2n-1)^2\pi^2/4\right)t\right)\cos\left((n-1/2)\pi y\right) \times \left(\frac{2P_0\,(-1)^{n-1}}{(2n-1)\,\pi} - \frac{8P_0 y}{(2n-1)^2\pi^2}\cos\left((n-1/2)\pi y\right) - 2P_0\left(\frac{y^2}{(2n-1)\pi} - \frac{8}{(2n-1)^3\pi^3}\right)\sin\left((n-1/2)\pi y\right)\right). \tag{22}$$

Equation 22 is the overall transient velocity for the fluid flowing in parallel plates filled with the homogenous and isotropic porous medium as $Da \to \infty$. As can be seen from the equation, the overall transient velocity is dependent on the dimensionless time, the dimensionless pressure gradient, and the dimensionless transverse distance.

4 Temperature Distribution in a Saturated Porous Medium between Parallel Plates

As stated previously, the homogenous and isotropic porous medium between two large parallel plates is saturated with a fluid flowing in the axial direction and is assumed to be in the local thermodynamic equilibrium with the fluid. It is assumed that the thermophysical properties of the solid matrix and of the fluid are constant. The porosity and permeability are also assumed to be constant even close to the walls (see Mahmud and Fraser 2005 and references therein). For $x > 0$, there are constant wall temperatures specifically T_1 and T_2 for the bottom plate and the upper plate, respectively. The dimensionless velocity distributions, at least far enough downstream from the inlet so that the entrance length has been exceeded, can be computed from the equations given above.

In order to obtain the steady-state temperature distribution for a laminar flow of a Newtonian fluid confined in parallel plates filled with a homogenous and isotropic porous medium, the energy equation with the viscous dissipation terms in the axial direction has to be solved with the appropriate boundary conditions.

By utilizing the above dimensionless variables, the energy equation with viscous dissipation terms for the steady state in the axial direction is rewritten in the dimensionless form as follows:

$$Re\,\mathrm{Pr}\left(\delta u\frac{\partial\theta}{\partial x} + v\delta_u\frac{\partial\theta}{\partial y} + \delta^2 w\frac{\partial\theta}{\partial z}\right) = \delta^2\frac{\partial^2\theta}{\partial x^2} + \frac{\partial^2\theta}{\partial y^2} + \delta^2\frac{\partial^2\theta}{\partial z^2} + 2Ec\,\mathrm{Pr}\left\{\delta^2\left(\frac{\partial u}{\partial x}\right)^2 + \delta_u^2\left(\frac{\partial v}{\partial y}\right)^2 + \delta^3\left(\frac{\partial w}{\partial z}\right)^2\right\} + Ec\,\mathrm{Pr}\left\{\left(\frac{\partial u}{\partial y} + \delta\delta_u\frac{\partial v}{\partial x}\right)^2 + \delta^2\left(\frac{\partial u}{\partial z} + \delta\frac{\partial w}{\partial x}\right)^2\right.$$

$$+\delta^2\left(\delta_u\frac{\partial v}{\partial z}+\frac{\partial w}{\partial y}\right)^2\Bigg\}+\frac{Ec\,\mathrm{Pr}}{Da}\left(u^2+\delta_u^2v^2\right.$$
$$\left.+\delta^2w^2\right), \tag{23}$$

where $\theta=(T-T_1)/(T_2-T_1)$, $\mathrm{Pr}=\frac{\mu C_p}{k_f}$ and $Ec=\frac{u_0^2}{Cp\Delta T}$, $\delta=\frac{h}{\ell}$, $\delta_u=\frac{v_0}{u_0}\approx\frac{h}{\ell}$, θ is the dimensionless temperature, Pr the Prandtl number, and Ec the Eckert number.

Taking $Re<<1$ for a typical laminar flow regime and $\delta<<1$ for a typical planar geometry and $\delta_u<<1$ for a typical one-dimensional flow make, Eq. 23 reduces to the following equation.

$$\frac{\partial^2\theta}{\partial y^2}+Ec\,\mathrm{Pr}\left(\frac{\partial u}{\partial y}\right)^2+\frac{Ec\,\mathrm{Pr}}{Da}u^2=0. \tag{24}$$

Here, we followed a more systematic approach, namely, the order of magnitude of each term in the energy equation for the derivation of the one-dimensional approximate governing equation of a forced convective heat transfer for a Newtonian fluid flowing in the saturated porous medium between two large closely spaced parallel plates, and the resulting equation (Eq. 24) is solved by using the method of separation of variables subject to the following boundary conditions.

$$\theta=0\quad\text{at}\quad y=-1\quad\text{and}\quad\theta=1\quad\text{at}\quad y=1. \tag{25}$$

where, θ is the dimensionless temperature defined above. After the fluid is far downstream from the beginning of the entrance, one intuitively expects that the constant wall temperature will result in the constant temperature of the saturated porous medium in the axial direction. One further expects that the shape of the transverse temperature profiles will ultimately not undergo further change with increasing x.

Substituting the derivative of Eq. 12 with respect to y and the steady-state velocity expression (Eq. 12) into Eq. 24 gives the following equation:

$$\frac{\partial^2\theta}{\partial y^2}=-\frac{Br\,Da\,P_0^2}{2+e^{2/\sqrt{Da}}+e^{-2/\sqrt{Da}}}\left\{2\left(e^{2y/\sqrt{Da}}+e^{-2y/\sqrt{Da}}\right)+2+e^{2/\sqrt{Da}}+e^{-2/\sqrt{Da}}\right.$$
$$\left.-2\left(e^{1/\sqrt{Da}}+e^{-1/\sqrt{Da}}\right)\times\left(e^{y/\sqrt{Da}}+e^{-y/\sqrt{Da}}\right)\right\}. \tag{26}$$

The governing equation (Eq. 26) for the temperature distribution of a Newtonian fluid flow in a planar geometry filled with the homogenous and isotropic porous medium can be easily solved subject to boundary condition given by Eq. 25, and the solution of that equation is given by

$$\theta=\frac{Br\,Da\,P_0^2}{2+e^{2/\sqrt{Da}}+e^{-2/\sqrt{Da}}}\left\{(Da/2)\left(e^{2/\sqrt{Da}}+e^{-2/\sqrt{Da}}-\left(e^{2y/\sqrt{Da}}+e^{-2y/\sqrt{Da}}\right)\right)\right.$$
$$+\frac{1}{2}\left(2+e^{2/\sqrt{Da}}+e^{-2/\sqrt{Da}}\right)\left(1-y^2\right)+2Da\left(e^{1/\sqrt{Da}}+e^{-1/\sqrt{Da}}\right)$$
$$\left.\times\left(e^{y/\sqrt{Da}}+e^{-y/\sqrt{Da}}-\left(e^{1/\sqrt{Da}}+e^{-1/\sqrt{Da}}\right)\right)\right\}+\frac{1}{2}(1+y). \tag{27}$$

Equation 27 is the solution of energy equation for a flow in parallel plates filled with a homogenous and isotropic porous medium. As can be seen from Eq. 27, the temperature distribution is linearly dependent on the Brinkman number (the Eckert number × the Prandtl number) and depends on the square of pressure gradient. It is seen from Eq. 27 as $Da\to\infty$,

the dimensionless temperature goes to infinity which is an unrealistic value. In fact, Eq. 27 should represent the dimensionless temperature distribution valid for a Newtonian fluid flow in parallel plates at constant, but different temperature as $Da \to \infty$ since large values of the Darcy number correspond to flow of a Newtonian fluid clear of solid material in parallel plates. Therefore, the solution of energy equation, valid for the case of $Da \to \infty$, has to be determined for the problem at hand. The solution of the energy equation with viscous dissipation due to the velocity gradient as $Da \to \infty$ is given as follows:

$$\theta = \frac{Ec\,\mathrm{Pr}\,P_0^2}{4}\left[1 - y^4\right] + \frac{1}{2}\left(1 + y\right). \tag{28}$$

It is obvious that the first term in Eq. 28 comes from the viscous dissipation due to the velocity gradient and the second term comes from heat conduction in the transverse direction.

As stated earlier, it was assumed that the flow is laminar and fully developed and the phases are locally in thermal equilibrium. Therefore, the temperature profiles may retain the same shape along the axial direction.

After obtaining the temperature distributions for the limiting cases of the Darcy number, one can analyze the irreversibility of the process by applying the second law of thermodynamics. The total entropy generation includes contributions due to heat conduction in the transverse direction and the viscous dissipation resulting from the velocity gradient of the fluid and the Darcy–Brinkman dissipation. In other words, heat transfer processes are generally accompanied by thermodynamic irreversibility or entropy generation. The generation of entropy may be due to a variety of sources, primarily heat transfer down temperature gradients, characteristic of convective heat transfer, and viscous dissipation.

5 Entropy Generation in a Porous Medium Saturated by Incompressible Fluid Confined in a Slit

Consider an incompressible fluid flowing in the x-direction in a horizontal parallel plate filled with a homogenous and isotropic porous medium. It is assumed that laminar viscous flow through the saturated porous medium between parallel plates subject to constant but different temperature takes place for fluid possessing constant physical properties (ρ, μ, k, C_P). Thus, the entropy generation is unavoidable due to conduction heat transfer through the fluid and viscous dissipation. If we consider a three-dimensional infinitesimal fluid element in a porous medium and consider the element as an open thermodynamic system subject to mass fluxes, energy transfer and entropy transfer interactions through a fixed control surface in the saturated porous medium, the volumetric rate of entropy generation for incompressible Newtonian fluid in Cartesian coordinates is given as follows (Bejan 1984; Pop and Ingham 2001):

$$\begin{aligned} S_G = {} & \frac{k_f}{T^2}\left[\left(\frac{\partial T}{\partial \tilde{x}}\right)^2 + \left(\frac{\partial T}{\partial \tilde{y}}\right)^2 + \left(\frac{\partial T}{\partial \tilde{z}}\right)^2\right] + \frac{\mu}{T}\left[\left(\frac{\partial \tilde{u}}{\partial \tilde{x}}\right)^2 + \left(\frac{\partial \tilde{v}}{\partial \tilde{y}}\right)^2 + \left(\frac{\partial \tilde{w}}{\partial \tilde{z}}\right)^2\right] \\ & + \frac{\mu}{T}\left[\left(\frac{\partial \tilde{u}}{\partial \tilde{y}} + \frac{\partial \tilde{v}}{\partial \tilde{x}}\right)^2 + \left(\frac{\partial \tilde{u}}{\partial \tilde{z}} + \frac{\partial \tilde{w}}{\partial \tilde{x}}\right)^2 + \left(\frac{\partial \tilde{v}}{\partial \tilde{z}} + \frac{\partial \tilde{w}}{\partial \tilde{y}}\right)^2\right] \\ & + \frac{\mu}{TK}\left(\tilde{u}^2 + \tilde{v}^2 + \tilde{w}^2\right). \end{aligned} \tag{29}$$

The above equation (Eq. 19) indicates that the irreversibility or entropy generation results from the heat conduction in the spatial directions and the viscous dissipation due to velocity gradient and the Darcy–Brinkman dissipation.

In order to obtain the dimensionless entropy generation rate, the dimensionless variables defined previously are introduced to Eq. 29, and the resulting equation is given by

$$S_G = \frac{k_f \Delta T^2}{T^2 h^2}\left\{\delta^2\left(\frac{\partial\theta}{\partial x}\right)^2 + \left(\frac{\partial\theta}{\partial y}\right)^2 + \delta^2\left(\frac{\partial\theta}{\partial z}\right)^2 + \frac{2u_0^2\mu}{k_f\Delta T^2/T}\left[\delta^2\left(\frac{\partial u}{\partial x}\right)^2 + \delta_u^2\left(\frac{\partial v}{\partial y}\right)^2 + \delta^3\left(\frac{\partial w}{\partial z}\right)^2\right] + \frac{u_0^2\mu}{k_f\Delta T^2/T}\left[\left(\frac{\partial u}{\partial y} + \delta\delta_u\frac{\partial v}{\partial x}\right)^2 + \left(\delta\frac{\partial u}{\partial z} + \delta^2\frac{\partial w}{\partial x}\right)^2 + \left(\delta\delta_u\frac{\partial v}{\partial z} + \delta\frac{\partial w}{\partial y}\right)^2\right] + \frac{u_0^2\mu h^2}{K k_f\Delta T^2/T}\left(u^2 + \delta_u^2 v^2 + \delta^2 w^2\right)\right\}. \tag{30}$$

The dimensionless entropy generation rate equation can be rearranged and simplified by following a systematic approach, namely, the order of magnitude of each term in the equation for the derivation of the one-dimensional approximate governing entropy equation of a flow of a Newtonian fluid confined in the parallel plates filled with the homogenous and isotropic porous medium. Taking $\delta << 1$ for a typical planar geometry and $\delta_u << 1$ for a typical one-dimensional flow makes Eq. 30 reduce to the following equation.

$$\frac{S_G}{k_f\Delta T^2\left(T^2h^2\right)} = \left(\frac{\partial\theta}{\partial y}\right)^2 + \frac{E_c\,\mathrm{Pr}}{\Omega}\left(\frac{\partial u}{\partial y}\right)^2 + \frac{E_c\,\mathrm{Pr}}{\Omega Da}u^2, \tag{31}$$

where $\theta = (T - T_1)/(T_2 - T_1)$, $\Delta T = T_2 - T_1$, $\Omega = \Delta T/T_0$, $\mathrm{Pr} = C_p\mu/k_f$, $Ec = u_0^2/\left(C_p\Delta T\right)$, $Da = K/h^2$.

The term on the left-hand side of Eq. 31 is the dimensionless entropy generation rate and it is called as the local entropy generation number (Bejan 1979) and the denominator of the same term obtained from non-dimensionalizing the entropy equation is called as the characteristic entropy transfer rate ($S_{G,C}$) that is equal to

$$S_{G,C} = \left[\frac{k_f(\Delta T)^2}{h^2T_0^2}\right]. \tag{32}$$

Note that T in Eqs. 30 and 31 is taken to be equal to T_0 with the assumption that the temperature gradient in the y-direction is small (Bejan 1979). In other words, if θ in the expression of $T = T_1 + \theta\Delta T$ is much less than unity, T can be taken equal to T_1 that can be considered the absolute reference temperature and is equal to T_0. In some previous studies (for example Mahmud and Fraser 2005; Mitrovic and Maletic 2007), T was directly taken equal to T_0 without bothering T by writing in Eq. 30.

In the above equation, ΔT is the difference of temperatures between two plates ($T_2 - T_1$), T_0 is the absolute reference temperature, and h is the characteristic length that depends on the geometry and type of the problem. Here, it is equal to the half transverse distance between the two large plates. The dimensionless entropy generation rate for the flow of a Newtonian fluid in parallel plates filled with a homogenous and isotropic porous medium is given by rewriting Eq. 31 as follows:

$$N_S = \left(\frac{\partial\theta}{\partial y}\right)^2 + \frac{Br}{\Omega}\left(\frac{\partial u}{\partial y}\right)^2 + \frac{Br}{\Omega Da}u^2 \tag{33}$$

$$Br = \Pr \times Ec = \mu u_0^2/\left(k_f \Delta T\right),$$

where Br is the Brinkman number and Ω is the dimensionless temperature difference. Equation 33 can be expressed alternatively as follows:

$$N_S = N_Y + N_F + N_{DB}. \tag{34}$$

On the right-hand side of Eq. 34, the first term (N_Y) denotes the entropy generation by heat transfer due to the transverse conduction, the second term (N_F) accounts for the entropy generation due to velocity gradient dissipation, and the last term (N_{DB}) represents the entropy generation due to the Darcy–Brinkman dissipation.

As mentioned earlier, it was assumed that the flow is laminar and fully developed in the x-direction which requires that a one-dimensional flow occurs in the axial direction and a temperature gradient in the transverse direction.

The entropy generation number for the flow of a Newtonian fluid confined in a planar geometry filled with a homogenous and isotropic porous medium is obtained by substituting the derivatives of Eqs. 12 and 27 with respect to y and Eq. 12 itself into Eq. 33 as follows:

$$\begin{aligned} N_S = & \left[-\frac{Br\,Da\,P_0^2}{2+e^{2/\sqrt{Da}}+e^{-2/\sqrt{Da}}} \left\{ \sqrt{Da}\left(e^{2y/\sqrt{Da}} - e^{-2y/\sqrt{Da}}\right) + \left(2+e^{2/\sqrt{Da}}+e^{-2/\sqrt{Da}}\right) y \right.\right. \\ & \left.\left. - 2\sqrt{Da}\left(e^{1/\sqrt{Da}} + e^{-1/\sqrt{Da}}\right)\left(e^{y/\sqrt{Da}} - e^{-y/\sqrt{Da}}\right) \right\} + \frac{1}{2} \right]^2 \\ & + \frac{Br\,P_0^2\,Da}{\Omega} \left[\frac{e^{y/\sqrt{Da}} - e^{-y/\sqrt{Da}}}{e^{1/\sqrt{Da}} + e^{-1/\sqrt{Da}}} \right]^2 \\ & + \frac{Br\,P_0^2\,Da}{\Omega} \left[1 - \frac{e^{y/\sqrt{Da}} + e^{-y/\sqrt{Da}}}{e^{1/\sqrt{Da}} + e^{-1/\sqrt{Da}}} \right]^2. \end{aligned} \tag{35}$$

As can be seen from the above equation, as $Da \to \infty$ the dimensionless entropy generation rate goes to infinity that is an unrealistic value. Therefore, in order to obtain an equation of entropy generation number valid for the case of $Da \to \infty$, Eq. 33 has to be re-evaluated for the this case. As $Da \to \infty$, Eq. 33 becomes

$$N_S = \left(\frac{\partial \theta}{\partial y}\right)^2 + \frac{Br}{\Omega}\left(\frac{\partial u}{\partial y}\right)^2. \tag{36}$$

Similarly for the case of $Da \to \infty$, the entropy generation number for a flow of a Newtonian fluid confined in a planar geometry filled with a homogenous and isotropic porous medium is obtained by substituting the derivatives of Eqs. 13 and 28 with respect to y into Eq. 36 as follows:

$$N_S = Br^2 P_0^4 y^6 - Br\,P_0^2 y^3 + \frac{Br\,P_0^2}{\Omega} y^2 + \frac{1}{4}. \tag{37}$$

The equations obtained for entropy generation number for the flow of a Newtonian fluid confined in a planar geometry filled with a homogenous and isotropic porous medium at the extreme values of the Darcy number will be used for determining entropy generation profiles as functions of the Darcy number, the Brinkman number, the irreversibility distribution ratios, the dimensionless pressure drop, and the dimensionless transverse distance.

6 Results and Discussion

The transient velocity distribution and the steady-state temperature distribution by using the steady-state velocity and thus, the steady-state dimensionless entropy generation are analyzed for a Newtonian fluid flow in parallel plates filled with a homogenous and isotropic porous medium. The effects of the Darcy number, the Brinkman number, and the dimensionless pressure drop in the axial direction on the overall transient velocity distribution, the steady-state temperature distribution, and the entropy generation number are investigated by varying one of the effective parameter and keeping other two parameters constant at certain values.

The transient part velocity distribution of a Newtonian fluid flow in the narrow gap of two closely spaced parallel plates filled with a homogenous and isotropic porous medium is illustrated in Fig. 2 as a function of the dimensionless transverse distance at each value of the dimensionless time for constant values of the dimensionless pressure drop ($P_0 = -0.20$) and the Darcy number ($Da = 0.08$). The velocity values in Fig. 2 is computed from Eq. 18 by varying the transverse distance at each value of the dimensionless time and keeping the Darcy number and dimensionless pressure drop constant at values of 0.08 and -0.20, respectively. As can be seen in the figure, the tip of the transient part velocity profile goes back to the zero value with increasing dimensionless time. It can be said that the transient velocity reaches the steady-state velocity behavior for values of the dimensionless time larger than 0.26 at constant values of $P_0 = -0.2$ and $Da = 0.08$.

The transient part velocity profile as a function of the transverse distance at each value of the dimensionless time is shown in Fig. 3 for constant values of the Darcy number ($Da = 1.0$) and the dimensionless pressure drop ($P_0 = -0.20$). Figure 3 is also depicted with the aid of Eq. 18 in which the transient part velocity is computed by varying the dimensionless transverse distance and keeping the Darcy number and the dimensionless pressure drop constant at values of 1.0 and -0.20, respectively. In order to see the effect of the Darcy number on the transient part velocity profile, this figure is drawn for keeping all effective parameters constant except the value of Darcy number. If one compares Figs. 2 and 3, it will be seen that the transient part velocity profile in each figure quite differs from one another. The differences between these figures come only from the different values of the Darcy number. As

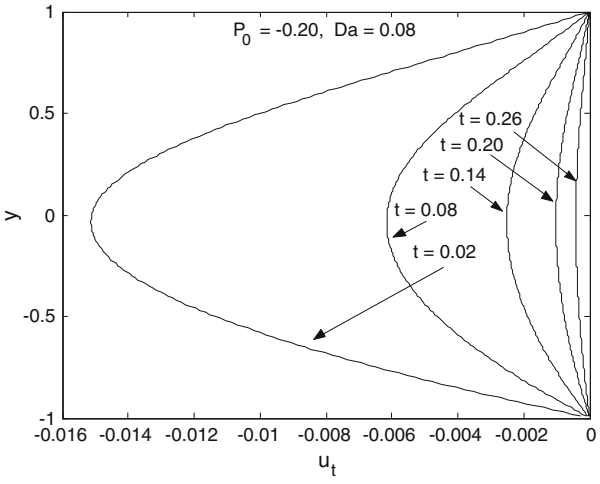

Fig. 2 Variations of the transient part velocity distribution with the dimensionless time at $P_0 = -0.2$ and $Da = 0.08$

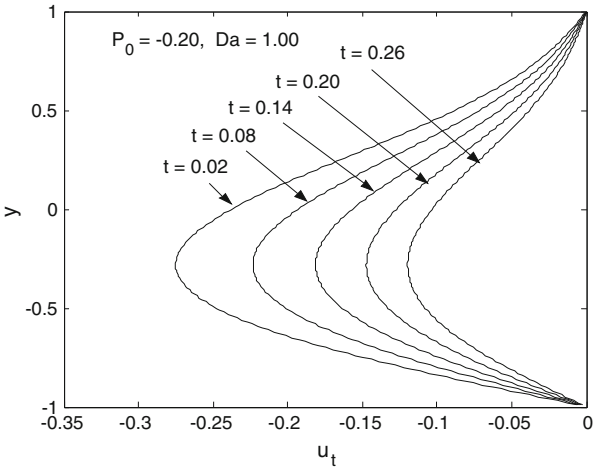

Fig. 3 Variations of the transient part velocity distribution with the dimensionless time at $P_0 = -0.2$ and $Da = 1.0$

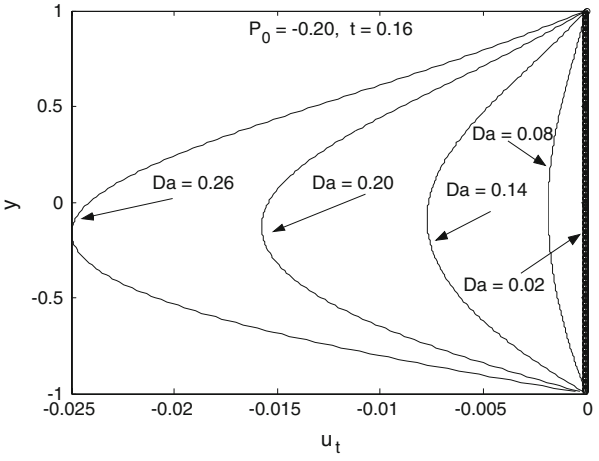

Fig. 4 The effect of the Darcy number on the transient part velocity distribution at $P_0 = -0.2$ and $t = 0.16$

can be seen in Fig. 3, the tip of the transient part velocity profile is far from the zero value at a value of $t = 0.26$. Therefore, it can be said that the transient part velocity is far to show the steady-state behavior at value of $P_0 = -0.20$, $Da = 1.0$, and $t = 0.26$. It can also be seen from the figure, that the tip of the transient velocity profiles at each value of the dimensionless time is not formed in the centerline of the channel; instead they take place in a region below the centerline of the channel.

The effect of the Darcy number on the transient part velocity profile is graphically illustrated in Fig. 4 for constant values of the dimensionless time ($t = 0.16$) and the dimensionless pressure drop ($P_0 = -0.20$). As seen from the figure, the magnitude of the transient part velocity profile decreases with decreasing the Darcy number. In other words, the tip of the transient part velocity profile moves back to reach zero value with decreasing the Darcy number for values of $P_0 = -0.20$ and $t = 0.16$. Furthermore, the tip of the velocity profile for lower values of the Darcy number is below the centerline of the planar geometry and moves toward the centerline with decreasing the Darcy number.

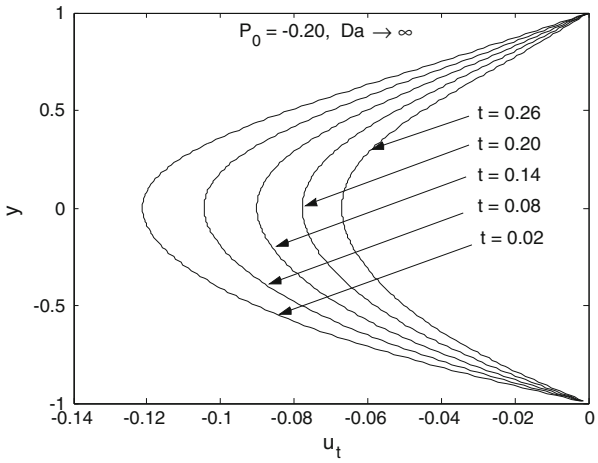

Fig. 5 Variations of the transient part velocity distribution with the dimensionless time at $P_0 = -0.2$ and as $Da \to \infty$

The effect of the dimensionless time on the transient part velocity profile at a constant value of the dimensionless pressure drop ($P_0 = -0.20$) and the case of $Da \to \infty$ is shown in Fig. 5 as a function of the dimensionless transverse distance. As seen in the figure, the magnitude of the transient part velocity profile decreases with increasing the dimensionless time. As expected, the transient part velocity profile reaches the steady-state velocity profile as $t \to \infty$. However, the transient part velocity profile for a maximum dimensionless time ($t = 0.26$) taken in the computation is far to reach the steady-state behavior at a value of $P_0 = -0.20$ and the case of $Da \to \infty$.

The overall transient velocity profile as a function of the transverse distance at each value of the dimensionless time is depicted in Fig. 6 for constant values of the Darcy number ($Da = 0.08$) and the dimensionless pressure drop ($P_0 = -1.20$). The overall transient velocity values drawn in Fig. 6 as a function of the transverse distance are computed from Eq. 19 by varying y and keeping the Darcy number and the dimensionless pressure drop constant at values of 0.08 and -1.20, respectively. As seen in the figure, the overall transient velocity at $t = 0.02$ takes a strange shape rather than a regular shape since this value of the dimensionless is too small for the problem at hand to show a regular shape for the velocity distribution. For a value of $t = 0.08$, the high velocity gradient near the walls and flat velocity distribution around the centerline of the channel are observed at constant values of $P_0 = -1.20$ and $Da = 0.08$. The flatness of the overall transient velocity decreases with increasing the dimensionless time at constant values of $P_0 = -1.20$ and $Da = 0.08$.

The effect of the Darcy number on the overall transient velocity profile is graphically illustrated in Fig. 7 as function of the transverse distance at constant values of the dimensionless time ($t = 0.5$) and the dimensionless pressure ($P_0 = -1.20$). The overall transient velocity depicted in Fig. 7 as a function of y is computed from Eq. 19 by varying the dimensionless transverse distance at each specified value of the Darcy number and keeping the dimensionless time and the dimensionless pressure drop constant at values of 0.5 and -1.20, respectively. As can be seen from the figure, the high velocity gradient near the walls and flat velocity distribution around the centerline of the planar geometry occur according to the values of the Darcy number at the specified constant values of the dimensionless time ($t = 0.50$) and the dimensionless pressure drop ($P_0 = -1.20$). The flatness of the overall transient velocity profile diminishes with increasing the Darcy number as evidenced in Fig. 7. In other words, the overall transient velocity profile approaches a regular shape of Poiseuille

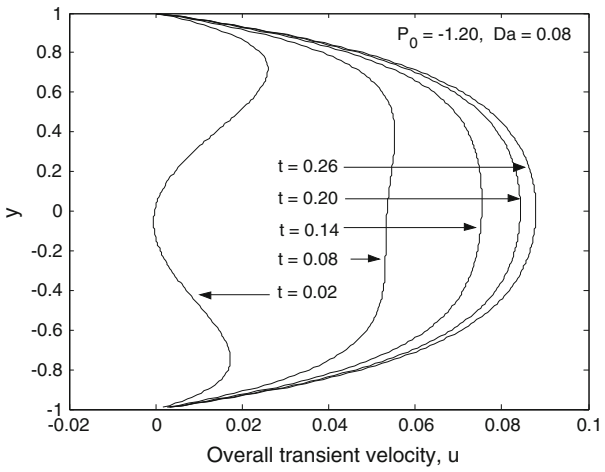

Fig. 6 Variations of the overall transient velocity distribution with the dimensionless time at $P_0 = -1.2$ and $Da = 0.08$

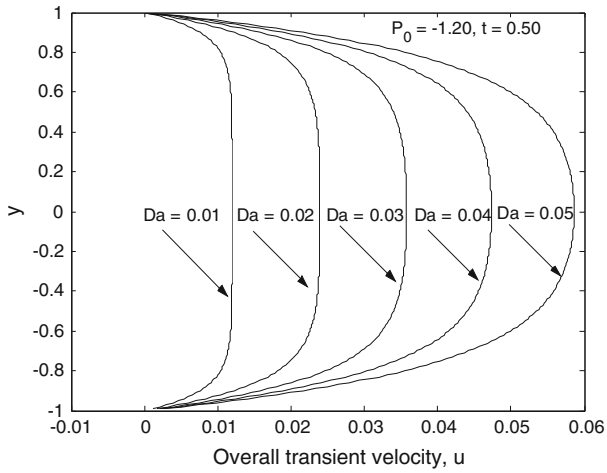

Fig. 7 The effect of the Darcy number on the overall transient velocity distribution at $P_0 = -1.2$ and $t = 0.50$

flow in a planar geometry as $Da \to \infty$ since the larger the value of Darcy number, the higher the permeability of the porous medium. At low values of the Darcy number ($Da \to 0$), the overall transient velocity profile is independent of the dimensionless transverse distance and slip flow occurs at, walls as evidenced in Fig. 7. The velocity of a Newtonian fluid confined in parallel plates filled with a homogenous and isotropic porous medium is hindered with decreasing the Darcy number.

The overall transient velocity of a Newtonian fluid flowing through the porous medium between two closely spaced parallel plates is sketched in Fig. 8 as a function of the dimensionless transverse distance at each specified value of the dimensionless time for a constant value of the dimensionless pressure drop ($P_0 = -1.20$) and the case of $Da \to \infty$. The velocity values illustrated graphically in this figure are computed from Eq. 22 by varying the dimensionless transverse distance at each specified dimensionless time for a constant value of the dimensionless pressure ($P_0 = -1.20$). It seems that the overall transient velocity profile takes a regular shape of the Poiseuille flow in a planar geometry after the dimensionless

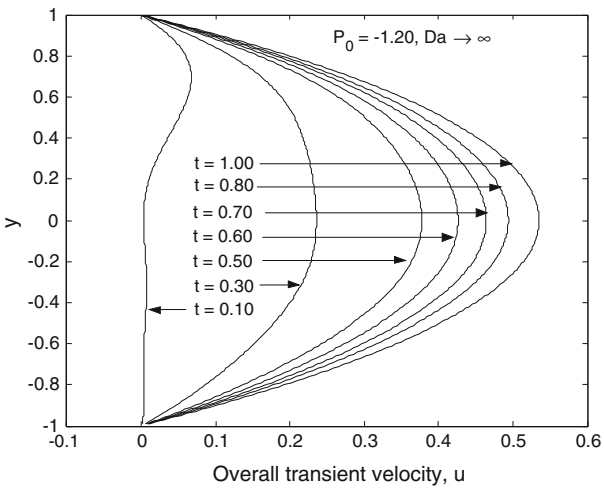

Fig. 8 Variations of the overall transient velocity distribution with the dimensionless time at $P_0 = -1.2$ and as $Da \to \infty$

time reaches a value around 0.50 for the problem at hand. As mentioned earlier, the overall transient velocity profile at the beginning does not gain a regular shape of the Poiseuille flow in parallel plates.

As stated previously, an incompressible Newtonian fluid with constant thermophysical properties of ρ, μ, k, C_P is flowing in laminar flow regime in parallel plates filled with a homogonous and isotropic porous medium. For $x > 0$, there are constant, but different wall temperatures specifically T_1 and T_2 for the bottom plate and the upper plate, respectively. The dimensionless velocity distributions, at least far enough downstream from the inlet so that the entrance length has been exceeded, can be computed from Eq. 12 that is a velocity expression valid at steady-state condition.

In order to obtain the temperature distribution for the incompressible Newtonian fluid flowing through the porous medium, the obtained velocity expression at the steady-state condition will be used in the energy equation with viscous dissipation consisting of the velocity gradient dissipation and the Darcy–Brinkman dissipation.

The effect of the Darcy number on the steady-state temperature distribution as a function of the transverse distance is shown in Fig. 9 for constant values of the dimensionless pressure ($P_0 = -1.20$) and the Brinkman number ($Br = 20$). The steady-state dimensionless temperature values in Fig. 9 are computed from Eq. 27 by changing the dimensionless transverse distance at each specified value of the Darcy number and keeping the Brinkman number and the dimensionless pressure constant at values of 20.0 and -1.20, respectively. As seen in the figure, the dimensionless steady-state temperature profile is linear at low values of the Darcy number; for instance, the dimensionless temperature profile between two plates is almost linear at a value of $Da = 0.01$. The linear temperature profile means the heat transfer is taking place between two plates by conduction and there is almost no energy generation due to viscous dissipation. This conclusion can be deduced from Eq. 24 with neglecting dissipation terms whose solution gives an expression for the dimensionless temperature, which is a linear function of y. An increase in the Darcy number results in a non-linear temperature distribution as evidenced in Fig. 9. The temperature of the porous medium between two large plates becomes higher than that of plates for values of the Darcy number higher than 0.02 at constant values of the Brinkman number ($Br = 20$) and the dimensionless pressure ($P_0 = -1.20$), and in this situation the heat transfer takes place from the porous medium to

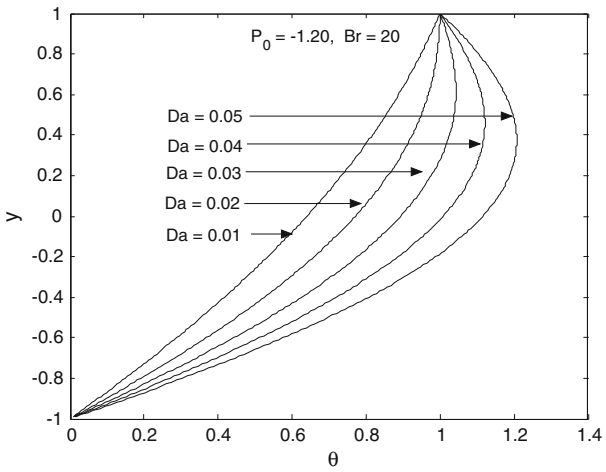

Fig. 9 Variations of the temperature distribution with the Darcy number at $P_0 = -1.2$ and $Br = 20.0$

both the plates. It is also seen from the figure, that the tip of the dimensionless temperature occurs at a region above the centerline of the planar geometry, which, we will see later, causes a lower entropy generation to take place at around the same region. The viscous dissipation due to the velocity gradient and the square of velocity (the Darcy–Brinkman dissipation) generates the energy in the saturated porous medium between two plates.

In order to determine the effect of the Brinkman number on the dimensionless steady, state temperature distribution, the temperature as a function of the dimensionless transverse distance at each specified value of the Brinkman is depicted in Fig. 10 for constant values of the Darcy number ($Da = 0.50$) and the dimensionless pressure ($P_0 = -1.20$). As seen in the figure, the dimensionless temperature profile is linear at a low value of the Brinkman number ($Br = 0.80$) for constant values of the Darcy number ($Da = 0.50$) and the dimensionless pressure ($P_0 = -1.20$). As stated previously, the linear temperature profile means the energy due to heat conduction in the transverse direction is dominant over the energy because of the viscous dissipation since the Brinkman number measures the relative importance of the energy due to the viscous dissipation to the energy because of heat conduction. As can be seen in the figure, the deviation from the linearity of the temperature profile increases with increasing the Brinkman number. It is also seen in the figure, that the temperature of the saturated porous medium between two plates is larger than that of the both plates for a value of the Brinkman number higher than 0.80 at constant values of $P_0 = -1.20$ and $Da = 0.50$. Therefore, heat transfer occurs from the porous medium saturated by a Newtonian fluid to the plates. As expected, the energy generation due to viscous dissipation increases with increasing the Brinkman number as evidenced in Fig. 10. If one compares Figs. 9 and 10, it will be seen that the effect of the Brinkman number on the dimensionless temperature distribution is more pronounced than that of the Darcy number for the considered values of the parameters. Figure 10 is in consistent with Fig. 9 since the temperature of the porous medium saturated by a Newtonian fluid increases with increasing the Darcy number that facilitates the fluid flow in the channel and thus, increases viscous dissipation. An increase in the Darcy number increases the permeability inside planar geometry that facilitates fluid flow.

Figure 11 illustrates the effect of the dimensionless pressure drop on the temperature distribution at constant values of the Brinkman number ($Br = 4.0$) and the Darcy number ($Da = 0.50$). Figure 11 is drawn with the aid of Eq. 27 by varying the dimensionless trans-

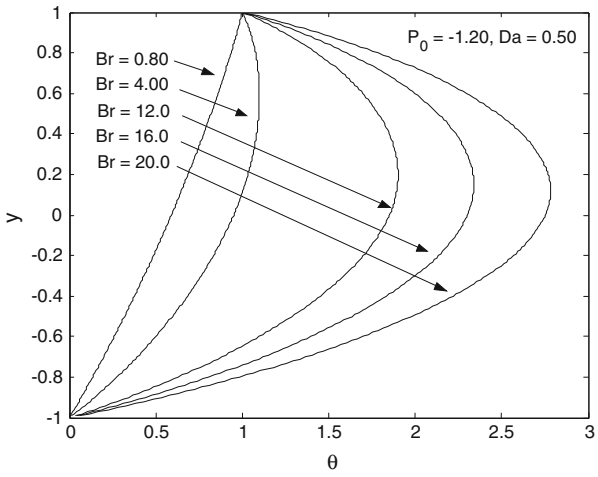

Fig. 10 Variations of the temperature distribution with the Brinkman number at $P_0 = -1.2$ and $Da = 0.50$

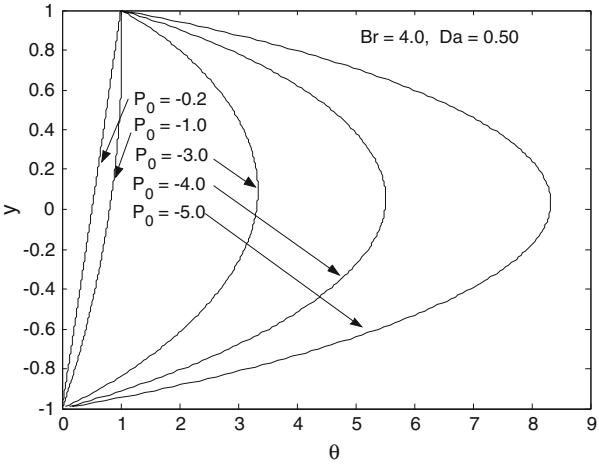

Fig. 11 Variations of the temperature distribution with the pressure drop at $Br = 4.0$ and $Da = 0.50$

verse distance at each specified value of the dimensionless pressure drop and keeping the Darcy number and the Brinkman number constant at values of 0.50 and 4.0, respectively. As can be seen in the figure, the linear temperature distribution between the two large plates occurs at a low value of the pressure drop ($P_0 = -0.20$). As explained earlier, the linear temperature profile corresponds to the energy due to heat conduction is dominant over the energy due to viscous dissipation. As seen in the figure, non-linearity in the temperature distribution increases with increasing the dimensionless pressure drop as increases of the Brinkman number and the Darcy number. The effect of the pressure drop on the temperature distribution is more pronounced than those of the Brinkman number and the Darcy number as evidenced in Fig. 11. In fact, an increase in the dimensionless pressure drop in the axial direction will make the fluid velocity to increase in the same direction and thus, increase the Brinkman number although in this study, the Brinkman number is assumed to be constant while the pressure drop increases. As stated previously, the effect of the pressure drop on the temperature distribution is more pronounced than that of the Brinkman number since the

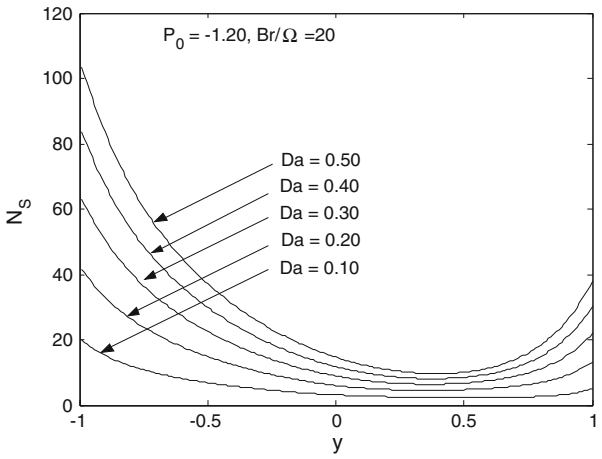

Fig. 12 Variations of the entropy generation with the Darcy number at $P_0 = -1.2$ and $Br/\Omega = 20.0$

square of the pressure drop in Eq. 27 lies as a numerator, while the Brinkman number itself lies as a numerator in the same equation.

After obtaining the velocity distribution and temperature distribution for a Newtonian fluid flow through the porous medium between two closely spaced parallel plates, the entropy generation can be easily analyzed for the problem at hand. In this context, in order to examine the effect of the Darcy number on the entropy generation, for constant values of the dimensionless pressure drop ($P_0 = -1.20$) and the irreversibility distribution ratio ($Br/\Omega = 20$), the entropy generation at each specified value of the Darcy number is depicted in Fig. 12 as a function of the dimensionless transverse distance. The entropy generation values in Fig. 12 is computed from Eq. 35 by changing y at each specified value of the Darcy number and keeping the pressure drop and the irreversibility distribution ratio constant at values of -1.20 and 20, respectively. As seen in the figure, the dimensionless entropy generation rate increases with increasing the Darcy number at all values of the transverse distance since the irreversibility due to fluid friction increases with increasing the Darcy number and, thus permeability. Furthermore, there is a lowest point of the entropy generation for each specified value of the Darcy number that is located between the centerline and the upper plate. Since the minimum temperature gradient results in the minimum entropy generation, this figure is in consistent with Fig. 9 in which the tip of the temperature profile at each specified value of the Darcy number was developed in a region between the centerline and the upper plate. As can be also seen in the figure, the entropy generation near the walls is larger than that in the porous medium saturated with a Newtonian fluid. Thus, it can be said that the larger velocity and temperature gradients occurring near the walls enhance the entropy generation in those regions. For the specified values of $P_0 = -1.20$ and $Br/\Omega = 20.0$, the entropy generation at the lower plate is larger than that at the upper plate as evidenced in Fig. 12 that can be attributed to the temperature distribution inside the porous medium between parallel plates since the tip of the temperature distribution occurred at a region close to the upper plate. Moreover, the entropy generation for each specified value of the Darcy number indicates a similar trend at constant values of the dimensionless pressure ($P_0 = -1.20$) and the irreversibility ratio ($Br/\Omega = 20.0$).

The irreversibility distribution ratio (Br/Ω) is an important parameter in heat transfer processes and measures the relative importance of the entropy generation due to viscous effect to the temperature gradient entropy generation. Therefore, in order to evaluate the effect of the

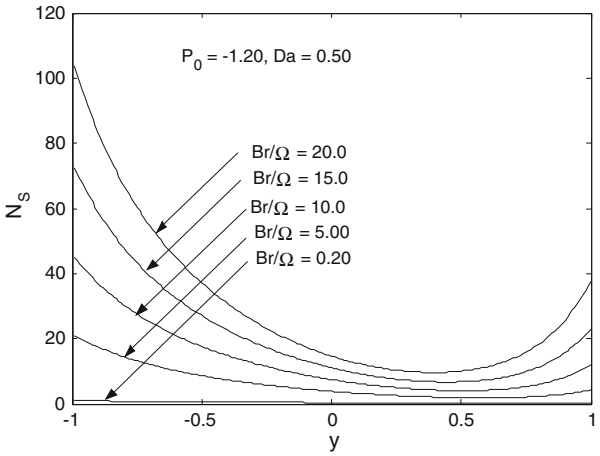

Fig. 13 Variations of the entropy generation with the irreversibility distribution ratio (Br/Ω) at $P_0 = -1.2$ and $Da = 0.50$

irreversibility distribution ratio (Br/Ω) on the entropy generation, for constant values of the dimensionless pressure drop $(P_0 = -1.20)$ and the Darcy number $(Da = 0.50)$, the entropy generation number as a function of the dimensionless transverse distance is illustrated in Fig. 13 at each specified value of Br/Ω . The entropy values in Fig. 13 are computed from Eq. 35 by varying y and keeping the dimensionless pressure drop and the Darcy number constant at values of -1.20 and 0.5, respectively. As seen in the figure, the entropy generation increases with increasing the irreversibility distribution ratio (Br/Ω) at constant values of $P_0 = -1.20$ and $Da = 0.50$. At a low value of $(Br/\Omega = 0.20)$, the entropy generation number is independent of the transverse distance, which corresponds to the energy due to heat conduction and is dominant over the energy because of viscous dissipation since the irreversibility distribution ratio measures the relative importance of the entropy generation due to viscous effect to temperature gradient entropy generation. There is a lowest point of the entropy generation at each specified value of the irreversibility distribution ratio except a value of $(Br/\Omega = 0.20)$. At high values of the irreversibility distribution ratio, each wall acts as a strong concentrator of irreversibility due to the high velocity and temperature gradients occuring near the walls.

The entropy generation as a function of the transverse distance at each specified value of the dimensionless pressure drop is sketched in Fig. 14 for constant values of the Darcy number $(Da = 0.50)$ and the irreversibility distribution ratio $(Br/\Omega = 5.0)$. As can be seen in the figure, the entropy generation increases with increasing the dimensionless pressure drop in the axial direction for constant values of Da and Br/Ω . The effect of the dimensionless pressure drop on the entropy generation number is more pronounced than those of the Darcy number and the irreversibility distribution ratio as evidenced in Figs. 12, 13, and 14. The similar conclusion can be deduced from Eq. 35 in which the square of the pressure drop lies as numerator, while the Darcy number and the irreversibility distribution ratio just themselves lie as a numerator. At high values of the pressure drop, there is a lowest point of the entropy generation that is located in a region between the centerline of the channel and the upper plate, but close to the centerline as in the temperature distribution (see Fig. 11), which may correspond to the minimum velocity gradient. Furthermore, the entropy generation rate is independent of the transverse distance at the low values of the pressure drop $(P_0 = -0.20)$ at constant values of $Da = 0.50$ and $Br/\Omega = 5.0$. The entropy generation at high values of

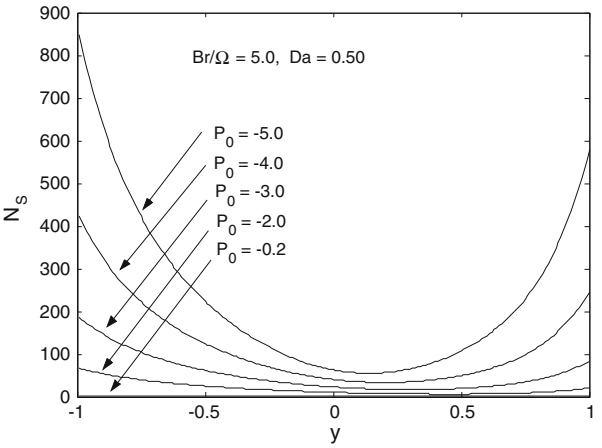

Fig. 14 Variations of the entropy generation with the pressure drop at $Da = 0.50$ and $(Br/\Omega) = 5.0$

the pressure is larger near the walls than inside the porous medium between parallel plates because of the high velocity and temperature gradients.

7 Conclusions

The flow of a Newtonian fluid confined in parallel plates filled with a homogenous and isotropic medium is analyzed in terms of determining the velocity, the temperature, and the entropy distributions as function of the effective process parameters such as the Darcy number, the Brinkman number, the irreversibility distribution ratio, and the pressure drop. In this context, the one-dimensional analytical expressions for the unsteady-state and the steady-state velocity of an incompressible Newtonian fluid flowing through the porous medium in parallel plates are derived by simplifying momentum equations by using the order of the magnitude of each term. Also the one-dimensional analytical expressions for the temperature and entropy generation are derived by considering the order of the magnitude of each term in the energy equations and solved analytically.

It is observed that the velocity of a Newtonian fluid flowing through the porous medium in a planar geometry hinders with decreasing the Darcy number and thus, the energy generation due to velocity gradient viscous dissipation and the Darcy–Brinkman viscous dissipation decreases. At small values of the Darcy number ($Da \to 0$), the velocity profile is independent of the transverse distance and the slip flow takes place on the walls while at the larger values of the Darcy number ($Da \to \infty$), the velocity profile takes a regular shape of the Poiseuille flow in a channel.

It is also observed that the variation of the temperature with the transverse distance is linear between the two plates at small values of the Darcy number. The deviations from the linearity of temperature distribution increase with increasing the Darcy number and thus, the temperature of the porous medium becomes higher than that of both the plates and heat transfer occurs from the medium to both the plates. The identical trend with different magnitude in the temperature distribution is observed for the cases of the pressure drop and the Brinkman number. The temperature distribution at low values of the pressure drop and the Brinkman number is found to be a linear function of y between the two plates, while it is found to be a non-linear function of y at larger values of those parameters.

The entropy generation distribution is not independent of the velocity and the temperature distributions. At low values of the Darcy number ($Da \rightarrow 0$), the entropy generation profile is observed to be independent of the transverse distance and the entropy generation increases with increasing the Darcy number at certain constant values of other parameters. It is also observed that the entropy generation increases with increasing the irreversibility distribution ratio, at the specified constant values of the other effective process parameters and at low values of the irreversibility distribution ratio, the entropy generation profile is independent of y. The variations of the pressure drop affect the entropy generation profile in a similar way that was observed for the Darcy number and the irreversibility distribution ratio.

References

Al-Hadhrami, A.K., Elliot, L., Ingham, D.B.: A new model for viscous dissipation in porous media across a range of permeability values. Transp. Porous Media **53**, 117–122 (2003). doi:10.1023/A:1023557332542

Bejan, A.: A study of entropy generation in fundamental convective heat transfer. J. Heat Transf. **101**, 718–725 (1979)

Bejan, A.: Convective Heat Transfer. Wiley, New York (1984)

Bejan, A., Dincer, I., Lorente, S., Miguel, A.F., Reis, A.H.: Porous and Complex Flow Structures in Modern Technologies. Springer, New York (2004)

Denn, M.M.: Process Fluid Mechanics. Prentice-Hall, New Jersey (1980)

Fang, T.: Further discussion on the incompressible pressure-driven flow in a channel with porous walls. Int. Comm. Heat Mass Transf. **31**, 487–500 (2004). doi:10.1016/S0735-1933(04)00030-2

Haji-Sheikh, A., Vafai, K.: Analysis of flow and heat transfer in porous media imbedded inside various shaped ducts. Int. J. Heat Mass Transf. **47**, 1889–1905 (2004). doi:10.1016/j.ijheatmasstransfer.2003.09.030

Haji-Sheikh, A., Nield, D.A., Hooman, K.: Heat transfer in the thermal entrance region for flow through rectangular porous passages. Int. J. Heat Mass Transf. **49**, 3004–3015 (2006). doi:10.1016/j.ijheatmasstransfer.2006.01.040

Hooman, K., Haji-Sheikh, A.: Analysis of heat transfer and entropy generation for a thermally developing Brinkman-forced convection problem in rectangular duct with isoflux walls. Int. J. Heat Mass Transf. **50**, 4180–4194 (2007). doi:10.1016/j.ijheatmasstransfer.2007.02.036

Hooman, K., Gurgenci, H., Merrikh, A.A.: Heat transfer and entropy generation optimization of forced convection in porous-saturated ducts of rectangular cross-section. Int. J. Heat Mass Transf. **50**, 2051–2059 (2007). doi:10.1016/j.ijheatmasstransfer.2006.11.015

Ingham, D.B., Pop, I.: Transport Phenomena in Porous Media III. Elsevier, Oxford (2005)

Kamışlı, F.: Pressure-driven laminar flow of a non-Newtonian fluid in a slit with wall suction or injection. Chem. Eng. Process. **47**, 585–595 (2008). doi:10.1016/j.cep.2006.11.012

Kaviany, M.: Laminar flow through a porous channel bounded by isothermal parallel plates. Int. J. Heat Mass Transf. **28**, 851–858 (1985)

Mahmud, S., Fraser, R.A.: Flow, thermal and entropy generation characteristics inside a porous channel with viscous dissipation. Int. J. Therm. Sci. **44**, 21–32 (2005). doi:10.1016/j.ijthermalsci.2004.05.001

Mitrovic, J., Maletic, B.: Heat transfer with laminar flow forced convection in a porous channel exposed to a thermal asymmetry. Int. J. Heat Mass Transf. **50**, 1106–1121 (2007). doi:10.1016/j.ijheatmasstransfer.2006.06.046

Mohammad, A.A.: Heat transfer enhancement in heat exchangers fitted with porous media. Part, I.: constant wall temperature. Int. J. Therm. Sci. **42**, 385–395 (2003). doi:10.1016/S1290-0729(02)00039-X

Morosuk, T.V.: Entropy generation in conduits filled with porous medium totally and partially. Int. J. Heat Mass Transf. **48**, 2548–2560 (2005). doi:10.1016/j.ijheatmasstransfer.2005.01.018

Nield, D.A.: Resolution of a paradox involving viscous dissipation and nonlinear drag in a porous medium. Transp. Porous Media **41**, 349–357 (2000)

Nield, D.A., Bejan, A.: Convection in Porous Media. 3rd edn. Springer, New York (2006)

Nield, D.A., Junqueira, S.L.M., Lage, J.L.: Forced convection in a fluid-saturated porousmedium channel with isothermal or isoflux boundaries. J. Fluid Mech. **322**, 201–214 (1996). doi:10.1017/S0022112096002765

Nield, D.A., Kuznetsov, A.V., Xiong, M.: Thermally developing forced convection in a porous medium: parallel plate channel with walls at uniform temperature, with axial conduction and viscous dissipation effects. Int. J. Heat Mass Transf. **46**, 643–651 (2003)

Pop, I., Ingham, D.B.: Convective Heat Transfer: Mathematical and Computational Modeling of Viscous Fluids and Porous Media. Pergamon, Oxford (2001)
Schlicting, H., Gersten, K.: Boundary Layer Theory. 8th Revised and Enlarged edn. (English). Springer-Verlag, New York (2000)
Vafai, K.: Handbook of Porous Media. 2nd edn. Taylor & Francis, New York (2005)
Vafai, K., Kim, S.J.: Forced convection in a channel filled with a porous medium: an exact solution. ASME J. Heat Transf. **111**, 1103–1106 (1989)